

Statistics of overtakes by a tagged agent

Santanu Das,¹ Deepak Dhar,² and Sanjib Sabhapandit¹

¹Raman Research Institute, Bangalore 560080, India

²Indian Institute of Science Education and Research (IISER), Pune 411008, India

(Dated: February 17, 2022)

We consider a one-dimensional infinite lattice where at each site there sits an agent carrying a velocity, which is drawn initially for each agent independently from a common distribution. This system evolves as a Markov process where a pair of agents at adjacent sites exchange their positions with a specified rate, while retaining their respective velocities, only if the velocity of the agent on the left site is higher. We study the statistics of the net displacement of a tagged agent $m(t)$ on the lattice, in a given duration t , for two different kinds of rates: one in which a pair of agents at sites i and $i + 1$ exchange their sites with rate 1, independent of the velocity difference between the neighbors, and another in which a pair exchange their sites with a rate equal to their relative speed. In both cases, we find $m(t) \sim t$ for large t . In the first case, for a randomly picked agent, m/t , in the limit $t \rightarrow \infty$, is distributed uniformly on $[-1, 1]$ for all continuous distributions of velocities. In the second case, the distribution is given by the distribution of the velocities itself, with a Galilean shift by the mean velocity. We also find the large time approach to the limiting forms and compare the results with numerical simulations. In contrast, if the exchange of velocities occurs at unit rate, independent of their values, and irrespective of which is faster, $m(t)/t$ for large t has a gaussian distribution, whose width varies as $t^{-1/2}$.

The phenomenon of overtaking is ubiquitous in nature. It occurs naturally in all sorts of traffics, ranging from the vehicular traffic on highways [1] to the transport at the molecular scale by motor proteins [2, 3]. Animals in groups, overtake each other to move to a less risky position at the center of the group [4]. Overtaking also takes place in sedimentation of mixtures with polydisperse (different sizes, densities) particles falling (or rising) through a fluid under gravity [5]. In biological evolution, the population sizes of different genotypes overtake each other depending on their fitness [6–9]. In a completely different context, the real-time correlation functions in quantum interacting many body systems may be understood in terms of overtaking dynamics of particles [10, 11].

In spite of its widespread appearances, surprisingly, the statistics of overtakes has not been studied much. In this Letter, we investigate the statistics of overtakes for a tagged agent in a simple model of stochastic evolution of self-driven agents (e.g., vehicles, molecular motors, etc.) in one dimension. In an overtake event, an agent with a higher velocity crosses another agent with a lower velocity. We define the *net overtakings* for a tagged agent as the total number of agents that it overtakes minus the total number of agents that overtake it, in a given duration. We study the probability distribution of fluctuations in this quantity. Certainly, such statistics can provide useful information about the underlying traffic. In particular, in traffic engineering, to obtain flow data, one uses the *moving observer method*, where an observer in a test vehicle moves a fixed distance with a constant speed and counts the number of vehicles that it overtakes and the number of vehicles that overtake it [12]. In these studies, the fluctuations are usually large, but their systematic study is lacking [13].

In this Letter, we discuss a minimalist model, consisting of a collection of self-driven agents on a one-

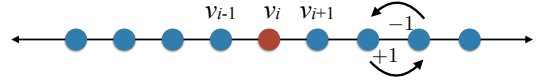


FIG. 1: Each site of a one-dimensional lattice is occupied by an agent (particle) with a certain velocity, and two neighboring particles interchange their positions with a specific rate. During the exchange, the net overtakings of the faster (slower) moving particle increases (decreases) by unity. The particle in red color is being tagged.

dimensional infinite line. We ignore the actual position of agents, and focus on the relative order. Then, to each site i of a lattice, with i ranging from $-\infty$ to ∞ , we associate a real random variable v_i , which is the velocity of the i -th agent along the track, starting from some fixed origin. Each agent is assigned a velocity, at the beginning, independent of others, from a common probability density function (PDF) $\rho(v)$. As agents overtake each other, their relative position with respect to other agents changes, but they retain their respective velocities with them, which are quenched random variables. Therefore, velocity v_i at a given site i , keeps changing as a function of time. In an exchange (overtake), the faster particle on the left overtakes a slower particle (see Fig. 1) on its right. Therefore the net overtakings in any time interval for a tagged agent equals its shift in position m in that interval on the lattice.

Here we consider two different cases for the exchange rates. For an overtake event to take place, the velocity of the overtaking agent must be greater than that of the overtaken agent. In the first case, we set the rate of exchange for agents between two neighboring lattice sites i and $i + 1$ as $r = \theta(v_i - v_{i+1})$, where $\theta(v) = 1$ for $v > 0$ and 0 for $v \leq 0$, is the Heaviside theta function. In this case, $m(t)$, for a given tagged agent with velocity v in-

creases linearly with time, say as $m(t) \approx c(v)t$, and the mean rate of increase of m depends on v . This case is related to the totally asymmetric simple exclusion process (TASEP), with infinitely many classes of particles, and has been studied much in literature [14–19]. Interestingly, if the agent being tracked is picked at random in the beginning, then, the velocity v itself is a random variable, and on averaging over this, we show below that the probability distribution of the random variable $c(v)$ is independent of the initial distribution of velocities, and is uniformly distributed on $[-1, 1]$, for all continuous distributions of the velocities. In the second case, motivated by the consideration of cars on a highway, where the rate of overtaking between two agents is approximately proportional to their relative velocities, we take $r = \theta(v_i - v_{i+1})(v_i - v_{i+1})$. In this case also, $m(t)$ again increases linearly with t . However, the limiting PDF of $c = m/t$ is given by the PDF of v itself, with the Galilean shift $\langle v \rangle$.

We contrast this behavior with what happens to $m(t)$ if the exchange rates r to be independent of the velocities and uniform everywhere, and adjacent velocities are exchanged at equal rate (chosen as 1 here), without consideration of which is faster. In this case, it is easy to see that, a tagged agent performs a symmetric random walk (RW), which is well-studied in literature [20]. In this case, the net overtakings $m(t)$, in a given time t , has the diffusive scaling $m(t) \sim \sqrt{t}$ and PDF of the scaled variable $y = m/\sqrt{t}$, in the limit $t \rightarrow \infty$, is Gaussian.

In the overtaking dynamics, where the exchange occurs only when the faster agent goes to the right, the behavior is very different, as we proceed to show. We can consider both the models described above, by writing in general $r = \theta(v_i - v_{i+1})(v_i - v_{i+1})^\alpha$, where $\alpha = 0$ and 1 correspond to the first and second choices of the rates respectively.

First consider the case $\alpha = 0$. Our model is equivalent to a totally asymmetric simple exclusion process (TASEP), with infinitely many classes of particles. However, if we consider the motion of a single tagged agent, say starting at the origin, and having the quenched velocity v_0 , the dynamics of this particle only depends on where the adjacent site has a velocity greater, or less, than v_0 . Let the density of agents having velocity greater than v_0 be $\rho_+(v_0) = \int_{v_0}^{\infty} \rho(v)$. Then, the motion of this tagged agent is same as that of a single *second class* particle in a TASEP, starting on an initial uncorrelated background of density of first-class particle $= \rho_+(v_0)$, and holes with density $\rho_-(v_0) = 1 - \rho_+(v_0)$. In this case, the tagged (second class) particle moves with a velocity $\bar{c}(v_0) = 1 - 2\rho_+(v_0)$ [14]. Evidently, $\bar{c}(v_0)$ is bounded by ± 1 , with $\bar{c} \rightarrow \pm 1$ for $v_0 \rightarrow \pm\infty$ (or the upper and the lower supports respectively) and $\bar{c}(v_0^*) = 0$ for $\rho_+(v_0^*) = \rho_-(v_0^*) = 1/2$. Ignoring fluctuations around $\bar{c}(v_0)$, the variable c is random through $c = \bar{c}(v_0)$. There-

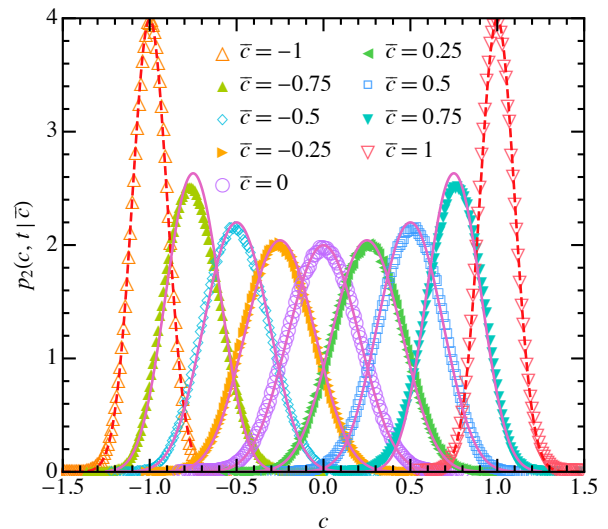


FIG. 2: (Color online). The points are numerical simulation results for the conditional PDF of scaled net overtakings $c = m(t)/t$ for given \bar{c} , for our first choice of the overtaking rate $r = \theta(v_i - v_{i+1})$. The initial velocities are drawn from uniform distribution on $[-1, 1]$. The dashed lines plot two Gaussian distributions centered around $\bar{c} = \pm 1$ respectively, with a variance t^{-1} . The solid line plots Eq. (4) for $\bar{c} = 0, \pm 0.25, \pm 0.5$ and ± 0.75 . In all the cases, $t = 100$.

fore, using $dc/dv_0 = -2\rho'_+(v_0) = 2\rho(v_0)$, we get

$$p(c) = \frac{\rho(v_0(c))}{|dc/dv_0|} = \frac{1}{2}. \quad (1)$$

Thus $c = m(t)/t$, in the limit $t \rightarrow \infty$, is uniformly distributed on $[-1, 1]$, for all continuous distributions $\rho(v)$, as claimed above.

A somewhat similar result was obtained earlier for TASEP with the step initial condition, and it was shown that a second class particle starting at the step, acquires a limiting speed that is uniformly distributed on $[-1, 1]$ [18, 19]. The corresponding result for our case is that when the initial velocities in our model with $\alpha = 0$ are in the descending order, $v_i > v_{i+1}$ for all i , an agent picked at random has a limiting speed, uniformly distributed on $[-1, 1]$.

One can also study fluctuations around the mean drift velocity $\bar{c}(v_0)$, for a given v_0 , at large, but finite, times t . The PDF of c at any time t (for any α) is given by

$$p(c, t) = \int_{-\infty}^{\infty} p_1(c, t|v_0) \rho(v_0) dv_0, \quad (2)$$

where $p_1(c, t|v_0)$ is the conditional PDF for a given v_0 . For $\alpha = 0$, as $p_1(c, t|v_0)$ is expected to depend on v_0 only through $\rho_+(v_0)$, or equivalently $\bar{c}(v_0)$, making a change of variable from v_0 to \bar{c} , eliminates $\rho(v_0)$ completely from Eq. (2),

$$p(c, t) = \frac{1}{2} \int_{-1}^1 p_2(c, t|\bar{c}) d\bar{c}, \quad (3)$$

where $p_2(c, t|\bar{c})$ is the conditional PDF for a given \bar{c} . Thus, not only the limiting distribution, but also the $p(c, t)$ at all time is independent of the velocity distribution $\rho(v)$. Note that, while obtaining Eq. (1), we have taken $p_2(c, t|\bar{c}) = \delta(c - \bar{c})$ by ignoring the fluctuations.

If we ignore the correlations between the jumps of the tagged particle at different times, then the typical fluctuations of c around the mean velocity $\bar{c}(v_0)$, at the scale of the standard deviation $\sigma_t = \sqrt{\langle [c - \bar{c}(v_0)]^2 \rangle} = t^{-1/2}$, are Gaussian. While this simple RW description holds good at an early time, the correlations between jumps build up at later times [21]. Eventually, it crosses over to $\sigma_t \propto \chi^{1/3} t^{-1/3}$ behavior [22–24] with $\chi = \rho_+(v_0)[1 - \rho_+(v_0)] = (1 - \bar{c}^2)/4$, and typical fluctuations are described by [23, 24]

$$p_2(c, t|\bar{c}) \simeq \frac{1}{4} (2\chi^{1/3} t^{-1/3})^{-1} G_{\text{scaling}}([c - \bar{c}]/[2\chi^{1/3} t^{-1/3}]), \quad (4)$$

where $G_{\text{scaling}}(w)$ is the scaling function associated with the spatio-temporal two-point correlation function of the TASEP with the Bernoulli product measure initial condition [23–27]. The crossover time $t_* \propto \chi^{-2}$.

At large times, since, $p_2(c, t|\bar{c})$ in Eq. (3) is peaked sharply around \bar{c} , the correction to Eq. (1) near the edges $c = \pm 1$, comes from $\bar{c} \rightarrow \pm 1$ respectively. In this case, t_* diverges. Hence, we can use the Gaussian form [see Fig. 2] $p_2(c, t|\bar{c}) \simeq \exp(-t[c - \bar{c}]^2/2)/\sqrt{2\pi t^{-1}}$ of the RW picture in Eq. (3). This yields

$$p(c, t) \simeq \frac{1}{4} \left[\text{erf} \left(\frac{(c+1)\sqrt{t}}{\sqrt{2}} \right) - \text{erf} \left(\frac{(c-1)\sqrt{t}}{\sqrt{2}} \right) \right], \quad (5)$$

where $\text{erf}(x) = (2/\sqrt{\pi}) \int_0^x e^{-y^2} dy$ is the error function. We compare this form with numerical results in Fig. 3 and find very good agreement. The agreement becomes even better, if the above Gaussian approximation is replaced by the large deviation form of the distribution for the RW [21]. The finite large time correction for the central region around $c = 0$ can be computed by using Eq. (4) [see Fig. 2] in Eq. (3) [see Fig. 3(e)].

Let us next consider the case $\alpha = 1$. For this, our model, in fact, corresponds to the infinite-species Karimipour model [28]. As in the $\alpha = 0$ case, here also, from numerical simulation we find that [21], the motion of the tagged agent with a given velocity v_0 can be well-approximated by a RW for $t \ll t_{\#}(v_0)$, where the characteristic time $t_{\#}(v_0)$ increases with v_0 going further away from the mean value $\langle v \rangle = \int_{-\infty}^{\infty} v\rho(v)dv$. The RW jumps to the right with the rate $\rho_R(v_0) = \int_{-\infty}^{v_0} (v_0 - v)\rho(v)dv$ and to the left with the rate $\rho_L(v_0) = \int_{v_0}^{\infty} (v - v_0)\rho(v)dv$. Therefore, the drift velocity $\bar{c}(v_0) = \rho_R(v_0) - \rho_L(v_0) = v_0 - \langle v \rangle$ and the standard deviation $\sigma_t = \sqrt{[\rho_L(v_0) + \rho_R(v_0)]/t}$. Even for $t \gg t_{\#}(v_0)$, from our simulation, we find that the typical fluctuations around its mean $\bar{c}(v_0)t$ are well-described by a Gaussian distribution, albeit with a standard deviation $\sigma_t \propto t^{-1/2}s(t)$. The factor $s(t)$ gives the correction to

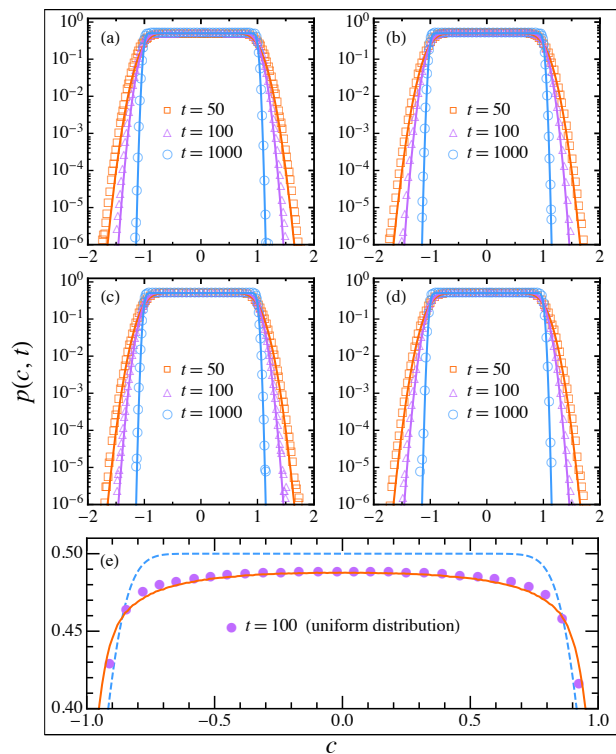


FIG. 3: (Color online). In (a), (b), (c), and (d): The points are numerical simulation results for the PDF of the scaled net overtakings $c = m(t)/t$ at different times, for our first choice of the overtaking rate $r = \theta(v_i - v_{i+1})$, where the initial velocities are chosen from (a) uniform, (b) Gaussian, (c) exponential, and (d) power-law distributions. The solid lines plot Eq. (5). In (e): The points are from a numerical simulation where the initial velocities are chosen from a uniform distribution on $[-1, 1]$ and $t = 100$. The solid line plots Eq. (3) computed by using Eq. (4) and the dashed line plots Eq. (5) for $t = 100$.

the standard RW result, which may be either a very small power-law $s(t) \sim t^{0.06\dots}$ or a logarithmic correction $s(t) \sim (\ln t)^\gamma$, and it is difficult to distinguish between the two behaviors based on our numerics [21] — as is often the case with marginal corrections [29–32]. Such logarithmic corrections have been found earlier in two-dimensional driven diffusive systems [22, 33–35] as well as for $1 + 1$ dimensional interface with cubic nonlinearity [36–39].

In the limit $t \rightarrow \infty$, ignoring the fluctuations around \bar{c} gives the limiting PDF $p(c) = \rho(c + \langle v \rangle)$, as announced above. The shift of the PDF by the mean is easily understood, as the overtaking dynamics depends only on the velocity differences. For the approach to this limiting distribution, we note that as in the $\alpha = 0$ case, the contributions to the large $|c|$ tails of $p(c, t)$ comes from large $|v_0 - \langle v \rangle|$ behavior of $p_1(c, t|v_0)$ in Eq. (2). Since $t_{\#}$ is large for large $|v_0 - \langle v \rangle|$, the tails of $p(c, t)$ can be computed by using a Gaussian distribution with mean $v_0 - \langle v \rangle$ and variance $[\rho_L(v_0) + \rho_R(v_0)]/t$ for $p_1(c, t|v_0)$ in

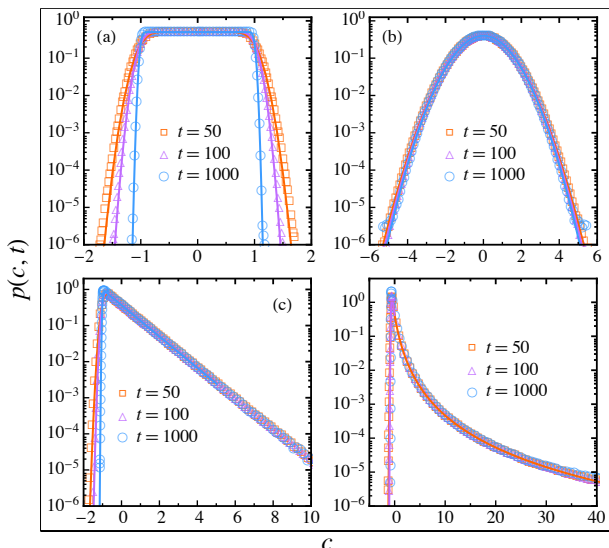


FIG. 4: (Color online). The points are numerical simulation results for the PDF of the scaled net overtakings $c = m(t)/t$ at different times, for the second choice of the overtaking rate $r = \theta(v_i - v_{i+1})(v_i - v_{i+1})$, where the initial velocities are chosen from (a) uniform, (b) Gaussian, (c) exponential, and (d) power-law distributions. The solid lines plot the theoretical results obtained from Eq. (6).

Eq. (2),

$$p(c, t) \simeq \int_{-\infty}^{\infty} dv_0 \rho(v_0) \frac{\sqrt{t}}{\sqrt{2\pi[\rho_L(v_0) + \rho_R(v_0)]}} \times \exp\left(-\frac{t[c + \langle v \rangle - v_0]^2}{2[\rho_L(v_0) + \rho_R(v_0)]}\right). \quad (6)$$

Evidently, $p(c, t)$ now depends on the form of $\rho(v_0)$ and the integral has to be carried out separately for each case. Figure 4 shows very good agreement between Eq. (6) and numerical simulation results for four different choices of $\rho(v_0)$.

It is interesting to note that the above RW picture for the overtaking dynamics, with the hopping rates $\rho_L(v_0)$ and $\rho_R(v_0)$, is exact for a model, known as the Jepsen gas [40], where the particles are non-interacting, distributed uniformly with unit density on the one-

dimensional (continuous) infinite line, and move ballistically with their velocities drawn independently for each particle from $\rho(v)$. This, for example, models the dynamics of cars on multi-lane highways at low densities.

As a side remark, in the case when the random velocity v takes only two distinct values, clearly, the value of α does not matter anymore, and the model corresponds to TASEP with identifying agents carrying one type of velocity as particles and the agents carrying the other type of velocity as holes. In this case, the tagged particle displacement $m(t)$ depends on the initial condition [41–44]. In particular, for independent and identically drawn initial velocities, a tagged particle performs a totally asymmetric RW in continuous time, where the fluctuations about the mean displacement are Gaussian and grows diffusively in time [45–48].

In conclusion, we have found two categories of overtaking behavior. In these cases, the net number of overtakes grows as t . We have also obtained the limiting distribution of the time-averaged overtaking rate, defined by the total number of net overtakings in a given time period divided by the total time, as well as the approach to the limiting distributions.

There are several interesting open directions for future research. First and foremost one is of course to analyze real data. Another question is whether there are other classes, and if any, how to identify them. Third, here we have studied only a single time property. However, one can study correlations between overtakes at different times or the overtaking dynamics itself as a process. Here, it is somewhat assumed that the density of agents is homogeneous in the real space, so that velocity is the only relevant variable for overtaking. One can explore the effect of inhomogeneity by considering a dilute case, where a finite number of sites, chosen randomly with a given density, are not occupied by agents (equivalently, occupied by agents having zero velocity). The simple picture presented in this Letter can serve as a stepping stone for future studies. The model on a finite line is also of interest. In this case, there are important end effects, and there are shock waves that start at the ends and travel inwards, and determine the qualitative behavior in the region deep inside for times of order of the system size. These will be discussed in a future publication.

-
- [1] D. Chowdhury, L. Santen, and A. Schadschneider, Phys. Rep. **329**, 199 (2000).
[2] M. Schliwa and G. Woehlke, Nature **422**, 759 (2003).
[3] R. Lipowsky, Y. Chai, S. Klumpp, S. Liepelt, and M. J. I. Müller, Physica A **372**, 34 (2006).
[4] A. Ward and M. Webster, *Sociality: The Behaviour of Group-Living Animals* (Springer 2016).
[5] R H Davis and A Acrivos, Ann. Rev. Fluid Mech. **17**, 91 (1985).
[6] J. A. G. M. de Visser and J. Krug, Nat. Rev. Genet. **15**, 480 (2014).
[7] J. Krug and C. Karl, Physica A **318**, 137 (2003).
[8] K. Jain and J. Krug, J. Stat. Mech. P04008 (2005).
[9] C. Sire, S. N. Majumdar, D. S. Dean, J. Stat. Mech., L07001 (2006).
[10] S. Sachdev and P. Young, Phys. Rev. Lett. **78**, 2220 (1997).
[11] K. Damle and S. Sachdev, Phys. Rev. Lett. **95**, 187201 (2005).
[12] P. Chakraborty and A. Das, *Principles of Transportation*

- Engineering* (Prentice-Hall, India 2004).
- [13] see, for example, C. A. O’flaherty and F. Simons, Australian Road Research Board conference, Canberra (1970) URL://arbbknowledge.com.
- [14] P. A. Ferrari, *Probab. Theo. Relat. Fields* **91**, 81 (1992).
- [15] P. A. Ferrari and C. Kipnis, *Ann. Inst. H. Poincaré Probab. Statist.* **31**, 143 (2005).
- [16] T. Mountford and H. Guiol, *Ann. Appl. Probab.* **15**, 1227 (2005).
- [17] P. A. Ferrari, C. Kipnis, and E. Saada, *Ann. Probab.* **19**, 226 (1991).
- [18] G. Amir, O. Angel, and B. Valkó, *Ann. Probab.* **39**, 1205 (2011).
- [19] O. Angel, A. Holroyd, and Dan Romik, *Ann. Probab.* **37**, 1970 (2009).
- [20] K. Pearson *Nature*. **72**, 294 (1905)
- [21] See Supplemental Material for more details.
- [22] H. van Beijeren, R. Kutner, and H. Spohn, *Phys. Rev. Lett.* **54**, 2026 (1985).
- [23] M. Prähofer and H. Spohn, In V. Sidoravicius, editor, In and out of equilibrium, *Prog. Probab.* **51**, 185 (Birkhäuser, Boston 2002).
- [24] P. L. Ferrari and H. Spohn, *Comm. Math. Phys.* **265**, 1 (2006).
- [25] J. Baik and E.M. Rains, *J. Stat. Phys.* **100**, 523 (2000).
- [26] M. Prähofer and H. Spohn, *J. Stat. Phys.* **115**, 255 (2004).
- [27] See M. Prähofer and H. Spohn (2003), <https://www-m5.ma.tum.de/KPZ> to numerically obtain $G_{\text{scaling}}(x)$.
- [28] V. Karimipour, *Phys. Rev. E* **59**, 205 (1999); *Europhys. Lett.* **47**, 304 (1999).
- [29] M.A. van der Hoef and D. Frenkel, *Phys. Rev. Lett.* **66**, 1591 (1991).
- [30] C.P. Lowe and D. Frenkel, *Physica A* **220**, 251 (1995).
- [31] M. Isobe, *Phys. Rev. E* **77**, 021201 (2008).
- [32] J. Krug, R. A. Neiss, A. Schadschneider, and J. Schmidt, *J Stat Phys* (2018), <https://doi.org/10.1007/s10955-018-1995-z>.
- [33] C. Landim, J. Quastel, M. Salmhofer and H.-T. Yau, *Comm. Math. Phys.* **244**, 455 (2004).
- [34] H.-T. Yau, *Ann. Math.* **159**, 377 (2004).
- [35] J. Quastel and B. Valkó, *Arch. Rational Mech. Anal.* **210**, 269 (2013).
- [36] B. Derrida, J. L. Lebowitz, E. R. Speer, and H. Spohn, *Phys. Rev. Lett.* **67**, 165 (1991); *J. Phys. A* **24**, 4805 (1991).
- [37] P. Devillard and H. Spohn, *J. Stat. Phys.* **66**, 1089 (1992).
- [38] M. Paczuski, M. Barma, S. N. Majumdar, and T. Hwa, *Phys. Rev. Lett.* **69**, 2735 (1992).
- [39] P.-M. Binder, M. Paczuski and M. Barma, *Phys. Rev. E* **49**, 1174 (1994).
- [40] D. W. Jepsen, *J. Math. Phys. (N.Y.)* **6**, 405 (1965).
- [41] H. van Beijeren, *J. Stat. Phys.* **63**, 47 (1991).
- [42] S. N. Majumdar and M. Barma, *Phys. Rev. B*, **44**, 5306 (1991).
- [43] A. Borodin, P. L. Ferrari, M. Prähofer, and T. Sasamoto, *J. Stat. Phys.* **129**, 1055 (2007).
- [44] T. Imamura and T. Sasamoto, *J. Stat. Phys.* **128**, 799 (2007).
- [45] A. de Masi and P. A. Ferrari, *J. Stat. Phys.* **38**, 603 (1985).
- [46] R. Kutner and H. van Beijeren, *J. Stat. Phys.* **39**, 317 (1985).
- [47] C. Kipnis, *Ann. Probab.*, **14**, 397 (1986).
- [48] Also remarked by H. Kesten, see in F. Spitzer, *Adv. Math.* **5**, 246 (1970).

Supplemental Material included from the next page.

Statistics of overtakes by a tagged agent: Supplemental material

Santanu Das,¹ Deepak Dhar,² and Sanjib Sabhapandit¹

¹*Raman Research Institute, Bangalore 560080, India*

²*Indian Institute of Science Education and Research (IISER), Pune 411008, India*

(Dated: April 17, 2018)

In the main text, we have considered a one-dimensional infinite lattice where at each site there sits an agent carrying a velocity, which is drawn initially for each agent independently from a common distribution $\rho(v)$. The system evolves by a Markovian dynamics where a pair of agents at adjacent sites i and $i + 1$ exchange their positions with the rate $r = \theta(v_i - v_{i+1})(v_i - v_{i+1})^\alpha$ where v_i is the velocity at site i before the exchange. The agents retain their respective velocities with them at all times, and hence, the velocity v_i at a given site i keeps changing with time. We have studied the statistics of the net displacement of a tagged agent $m(t)$ on the lattice, in a given duration t , for two different cases: $\alpha = 0$ and $\alpha = 1$. Here we provide additional materials to support the main text.

1. For the $\alpha = 0$ case, we have mentioned in the main text that the variance of the displacement of a tagged agent crosses over from the initial $\langle m^2 \rangle_c \propto t$ behavior to the long time behavior $\langle m^2 \rangle_c \propto t^{4/3}$, where the crossover time depends on the velocity v_0 of the tagged agent. Here we illustrate this in Fig. 1.
2. In Fig. 2 of the main text, we have illustrated that the conditional probability density function (PDF) $p_2(c, t|\bar{c})$ for $\bar{c} \rightarrow \pm 1$, is given by the Gaussian distribution, coming from the random walk description of the process, while at the central part $p_2(c, t|\bar{c})$ is described by Eq. (4) of the main text. Here instead, we look at the conditional PDF $p_1(c, t|v_0)$ itself at fix times for different values of v_0 . If v_0 is such that the characteristic time $t_*(v_0)$ is large compared to our observation times, the dynamics of the tagged agent can be described by random walk as shown by the two figures on the first row of Fig. 2. The Gaussian distribution describes the typical fluctuation for the displacement of a random walk only at the scale of \sqrt{t} about the mean [see the first figure on the first row of Fig. 2]— unless the jump distribution itself is Gaussian, where fluctuations of the displacement at all scales are also Gaussian. To confirm that the jump process at $t \ll t_*(v_0)$ is indeed well-described by the random walk, we also look at the large fluctuations at the scale of t , which are described by the large deviation form discussed in Sec. I below. The second figure on the first row of Fig. 2 indeed affirms this. In Fig. 2 of the main text, we have shown that for small \bar{c} , the conditional PDF $p_2(c, t|\bar{c})$, when shifted and scaled appropriately, is given by the scaling function $G_{\text{scaling}}(y)$, that is discussed in the main text. Here, in the figure on second row of Fig. 2, we illustrate that if v_0 is such that $t_*(v_0)$ is small compared to our observation times, the conditional PDF $p_1(c, t|v_0)$, when shifted and scaled appropriately, is given by the scaling function $G_{\text{scaling}}(y)$.
3. In Fig. 3 (a), (b), (c), and (d) of the main text, we have plotted the simulation results for the PDF of $c = m(t)/t$ for four choices of the velocity distributions (the exact form of the distributions are given in Sec. II below) and compared them with Eq. (5). We find very good agreement at large times. Note that Eq. (5) of the main text has been obtained by using a Gaussian distribution for $p_2(c, t|\bar{c})$. As mentioned above, and illustrated in Fig. 2, the large fluctuation are better described by the large deviation form of the PDF, which also include the typical fluctuations. Therefore, here we use the large deviation form Eq. (S8) in Eq. (3) of the main text to numerically obtain the PDF $p(c, t)$ and compare this with simulation results in Figure 3, which gives better agreement than Eq. (5) of the main text. This confirms that, the tails of $(p(c, t))$ indeed comes from the random walk description.
4. For the $\alpha = 1$ case, we have mentioned in the main text that the variance of the displacement of a tagged agent crosses over from the initial $\langle m^2 \rangle_c \propto t$ behavior to the long time marginally superdiffusive behavior. Here we illustrate this in Fig. 4.
5. In Fig. 5 we illustrate that at early times $t \ll t_{\#}(v_0)$, for the $\alpha = 1$ case also, the jump process of a tagged agent is described by the random walk. We do this by showing that the conditional PDF of the appropriately shifted and scaled displacement $y = (m - \bar{c}t)/\sqrt{t}$, for $t \ll t_{\#}(v_0)$ is Gaussian. We also look at the large fluctuations and find that it is given by the large deviation form Eq. (S9) for the random walk with the appropriate hopping rates. For $t \gg t_{\#}(v_0)$, the conditional PDF of the appropriately scaled displacement is again Gaussian — however, with a scaling marginally different from \sqrt{t} .
6. The exact anomalous scaling for the scaled displacement for $t \gg t_{\#}(v_0)$, for the $\alpha = 1$ case, is difficult to determine based on our numerics, as shown in Fig. 6.

7. In Fig. 7 we give additional support that the tails of $p(c, t)$ for $\alpha = 1$ case also comes from the random walk description of the jump process for an tagged agent. Here we magnify the tails part of the plots in Fig. (4) of the main text, and show that if we use the large deviation form for $p_1(c, t|v_0)$ to compute $p(c, t)$ in Eq. (2) of the main text, the simulation results for the tails agree even at smaller times.

I. LARGE DEVIATION FUNCTION OF FOR THE PDF OF THE DISPLACEMENT OF A RANDOM WALK ON A ONE-DIMENSIONAL LATTICE, EVOLVING IN CONTINUOUS TIME

Consider a random walk on a one-dimensional infinite lattice evolving as a continuous time Markov process. The random walker on the lattice jumps to right and left adjacent sites with homogeneous and time independent rates p_r and p_l respectively. The time evolution of the probability distribution $P(m, t)$ of the walker of being at the site m at time t is given by the master equation

$$\frac{d}{dt}P(m, t) = p_r P(m - 1, t) + p_l P(m + 1, t) - (p_r + p_l) P(m, t). \quad (S1)$$

We consider initial condition $P(m, 0) = \delta_{m,0}$. The characteristic function is given by

$$\tilde{P}(k, t) \equiv \langle e^{ikm} \rangle = e^{\lambda(k)t} \quad (S2)$$

where the cumulant generating function (CGF) is given by

$$\lambda(k) = p_r (e^{ik} - 1) + p_l (e^{-ik} - 1). \quad (S3)$$

Evidently, the n -th cumulant is

$$\langle m^n(t) \rangle_c = [p_r + (-1)^n p_l] t. \quad (S4)$$

The distribution at large time can be obtained by inverting the characteristic function using saddle-point approximation, which for the scaled variable $c = m/t$ yields

$$P(c, t) \simeq \sqrt{\frac{t}{2\pi}} \frac{e^{-t \phi(c)}}{\sqrt{\phi''(c)}} \quad (S5)$$

with large deviation function (LDF) [1]

$$\phi(c) = c \text{Log} \left[\frac{c + \sqrt{c^2 + 4p_r p_l}}{2p_r} \right] + (p_r + p_l) - \sqrt{c^2 + 4p_r p_l} \quad (S6)$$

and $\phi''(c) = \sqrt{c^2 + 4p_r p_l}$. By expanding around its average \bar{c} , one can also recover the well known Gaussian approximated result (GUS)

$$P(c, t) = \frac{1}{\sqrt{2\pi\sigma_t^2}} e^{-\frac{(c-\bar{c})^2}{2\sigma_t^2}} \quad (S7)$$

where $\bar{c} = \langle m(t) \rangle_c / t = p_r - p_l$ and its variance $\sigma_t^2 = \langle m^2(t) \rangle_c / t^2 = (p_r + p_l) / t$.

A. Case I : ($\alpha = 0$)

In this case, in the main text we have used the rates $p_r(v_0) \equiv \rho_+(v_0)$ and $p_l(v_0) \equiv \rho_-(v_0)$ for a tagged particle of velocity v_0 . By using these relations we have plotted the distribution associated with LDF and GUS in the first row of Fig. 2. Now, using the PDF of the form of Eq. (S5) with the fact $p_r(v_0) + p_l(v_0) = 1$, the conditional PDF $p_2(c, t|\bar{c})$ in the main text can be written as:

$$p_2(c, t|\bar{c}) = \sqrt{\frac{t}{2\pi}} \frac{e^{-t \phi(c, \bar{c})}}{\sqrt{\phi''(c, \bar{c})}} \quad (S8)$$

with $\phi(c, \bar{c}) = c \text{Log} \left[\frac{c + \sqrt{c^2 + 1 - \bar{c}^2}}{1 + \bar{c}} \right] + 1 - \sqrt{c^2 + 1 - \bar{c}^2}$ and $\phi''(c, \bar{c}) = \sqrt{c^2 + 1 - \bar{c}^2}$. Using this result in Eq.(3) in main text we numerically computed the exact tail behavior of the scaled net overtaking distribution $p(c, t)$ as shown in Fig. 3.

B. Case II : ($\alpha = 1$)

In this case, in the main text we have used $p_r(v_0) \equiv \rho_R(v_0)$ and $p_l(v_0) \equiv \rho_L(v_0)$ for a tagged particle of velocity v_0 . By using these relations we have plotted the distribution associated with LDF and GUS in the first row of Fig. 5. Now, using the PDF of the form of Eq. (S5) with the fact $p_r(v_0) + p_l(v_0) = \sigma^2(v_0)$, the conditional PDF $p_1(c, t|v_0)$ in the main text can be written as:

$$p_1(c, t|v_0) = \sqrt{\frac{t}{2\pi}} \frac{e^{-t \phi(c, v_0)}}{\sqrt{\phi''(c, v_0)}} \quad (\text{S9})$$

with $\phi(c, v_0) = c \text{Log} \left[\frac{c + \sqrt{c^2 + \sigma^4(v_0) - \bar{c}^2(v_0)}}{\sigma^2(v_0) + \bar{c}(v_0)} \right] + \sigma^2(v_0) - \sqrt{c^2 + \sigma^4(v_0) - \bar{c}^2(v_0)}$ and $\phi''(c, v_0) = \sqrt{c^2 + \sigma^4(v_0) - \bar{c}^2(v_0)}$.

Using this result alongside the explicit form velocity distribution $\rho(v_0)$ in Eq.(2) in main text we numerically computed the exact tail behavior of the scaled net overtaking distribution $p(c, t)$ as shown in Fig. 7.

II. THE FOUR VELOCITY DISTRIBUTIONS USED IN THE MAIN TEXT:

In the main text we have shown numerical results for four different velocity distributions. The distribution are respectively

$$(i) \quad \rho(v) = \frac{1}{2}; v \in [-1 : 1] \quad (\text{Uniform}), \quad (\text{S10})$$

$$(ii) \quad \rho(v) = \frac{e^{-\frac{v^2}{2}}}{\sqrt{2\pi}}; v \in [-\infty : \infty] \quad (\text{Gaussian}), \quad (\text{S11})$$

$$(iii) \quad \rho(v) = e^{-v}; v \in [0 : \infty] \quad (\text{Exponential}), \quad (\text{S12})$$

$$(iv) \quad \rho(v) = \frac{\nu}{v^{1+\nu}}; v \in [1 : \infty] \quad (\text{Power law}). \quad (\text{S13})$$

The first two distributions are symmetric while the last two are asymmetric with respect to the mean of the distribution $\langle v \rangle$. From the other viewpoint, the first three distributions have all finite moments while the last one have diverging moments. The behavior of the power-law distribution is completely characterized by its exponent $\nu > 0$. In the main text, for power-law, all the results have shown for $\nu = 2.5$.

[1] H. Touchette, Phys. Rep. **478**, 1 (2009).

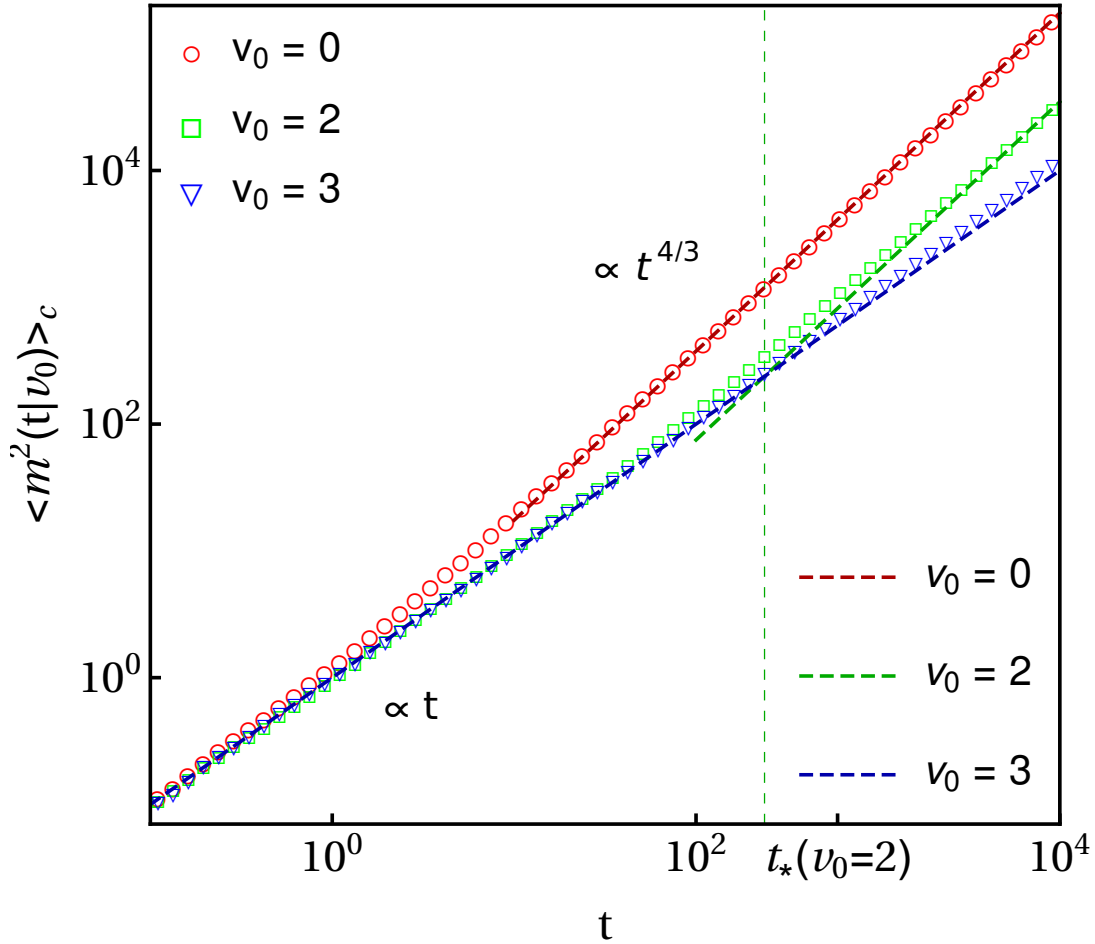


FIG. 1: Simulation results (shown by discrete points), illustrating the crossover from the initial $\propto t$ behavior to the long-time $\propto t^{4/3}$ behavior, for the variance of the displacement of the tagged particle for the $\alpha = 0$ case discussed in the main text. Three different values of the tagged velocity $v_0 = 0, 2$, and 3 are considered while the initial velocities of the other particles are drawn independently from a Gaussian distribution. The finite size effects do not show up till the final measurement time considered in the simulations, for a system of size $N = 2 \times 10^3$ with periodic boundary condition. For $v_0 = 0$ an anomalous growth $\propto t^{4/3}$ is clearly noticeable. The result for the intermediate velocity $v_0 = 2$ is showing a transition from the initial $\propto t$ behavior to the long-time $\propto t^{4/3}$ behavior. The third one $v_0 = 3$ mostly shows the linear growth $\propto t$, with a hint of the crossover towards the end. The dashed lines plot the analytical results which show a good agreement with the corresponding numerical results. The vertical dashed line is showing an approximate transition time $t_*(v_0)$ between the initial linear growth to the long-time non-linear one for velocity $v_0 = 2$.

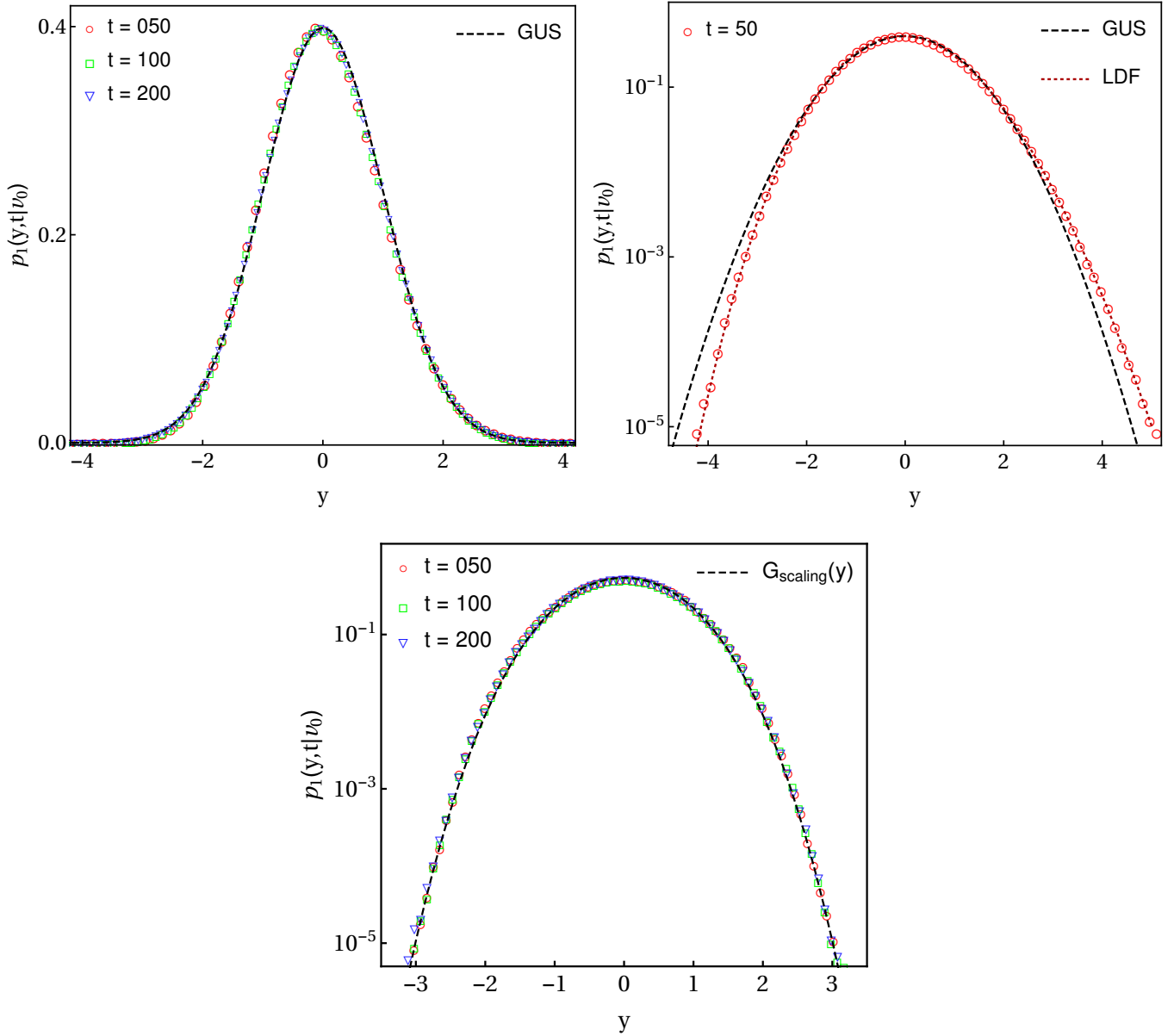


FIG. 2: Conditional PDF of the displacement $m(t)$ of the tagged particle with a given velocity v_0 in the two different limits (i) $t \ll t_*(v_0)$ (the two figures on the first row) and (ii) $t \gg t_*(v_0)$ (the figure on the second row), for the $\alpha = 0$ case discussed in the main text. To satisfy those limits we have conveniently considered the tagged velocity $v_0 = 3$ for the two figures on the first row and $v_0 = 0$ for the figure on the second row. In the first figure on the first row, the simulation results, denoted by points, for the PDF of the scaled displacement $y \propto (m - \bar{c}t)/\sqrt{t}$, are plotted together with a Gaussian distribution denoted by the dashed line. In the second figure on the first row, we use log-linear scale to show that a large fluctuations deviates from the Gaussian (shown by the dashed line), which are better described by the large deviation result shown by the dotted line. The figure on the second row demonstrates that in the opposite limit $t \gg t_*(v_0)$, with the appropriate scaling $y \propto t^{-2/3}(m - \bar{c}t)$, the PDFs for different times collapse onto the scaling function $G_{\text{scaling}}(y)$ (shown by dashed line) that is discussed in the main text.

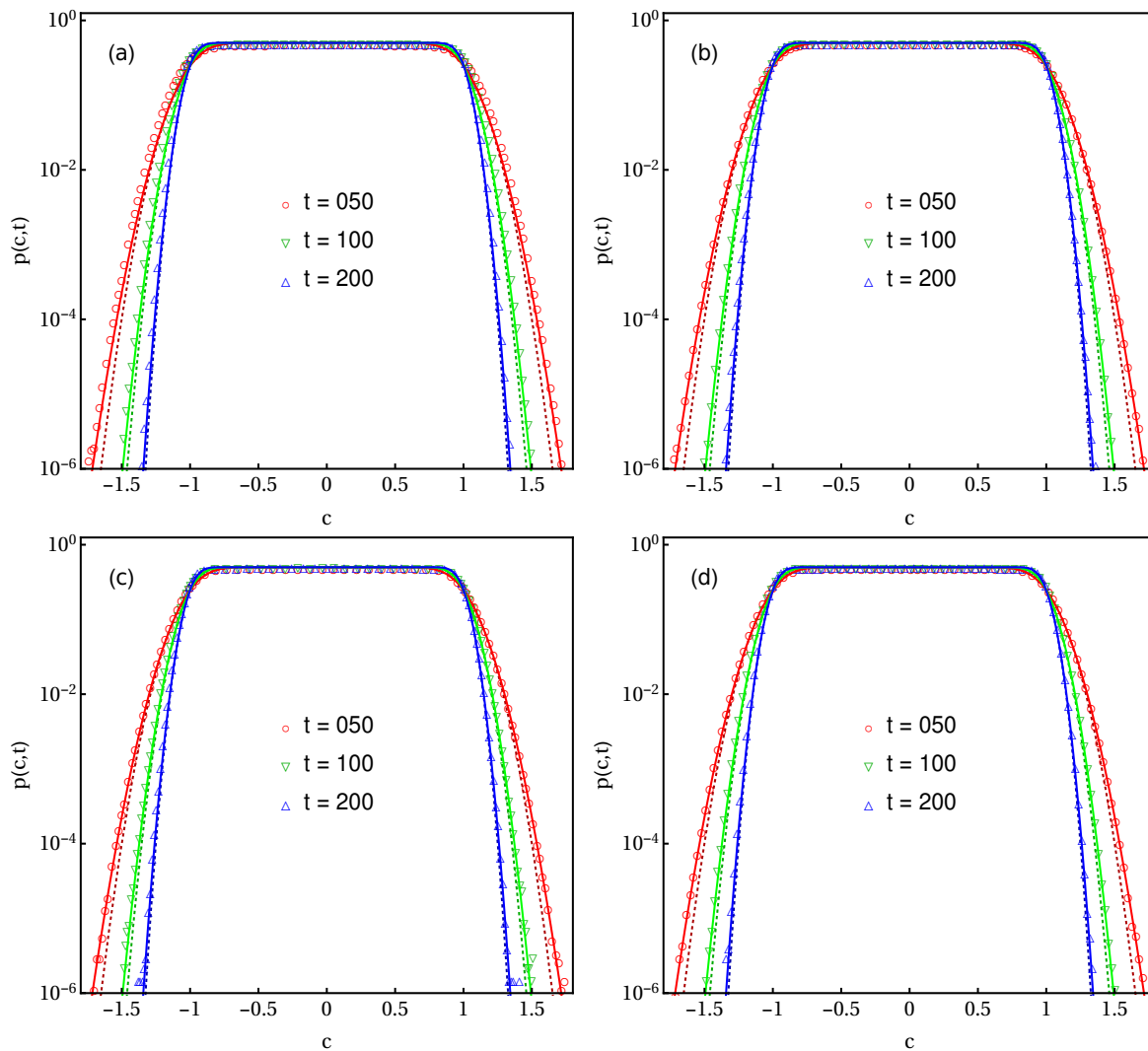


FIG. 3: Probability density function $p(c, t)$ of the scaled net overtakings $c = m(t)/t$ are plotted at three different times, for $\alpha = 0$ case discussed in the main text, with four different choices of the initial velocity distribution, namely, (a) uniform (b) Gaussian (c) exponential and (d) power-law distributions. The discrete points in each plot are the simulation results, which show very good agreements with the results coming from the analysis of the large deviation form of the conditional distribution $p_2(c, t|v_0)$ (as shown by the bold lines). The corresponding results coming from the Gaussian approximation, are plotted by the dashed lines, for which the agreements at the tails improve as t becomes larger.

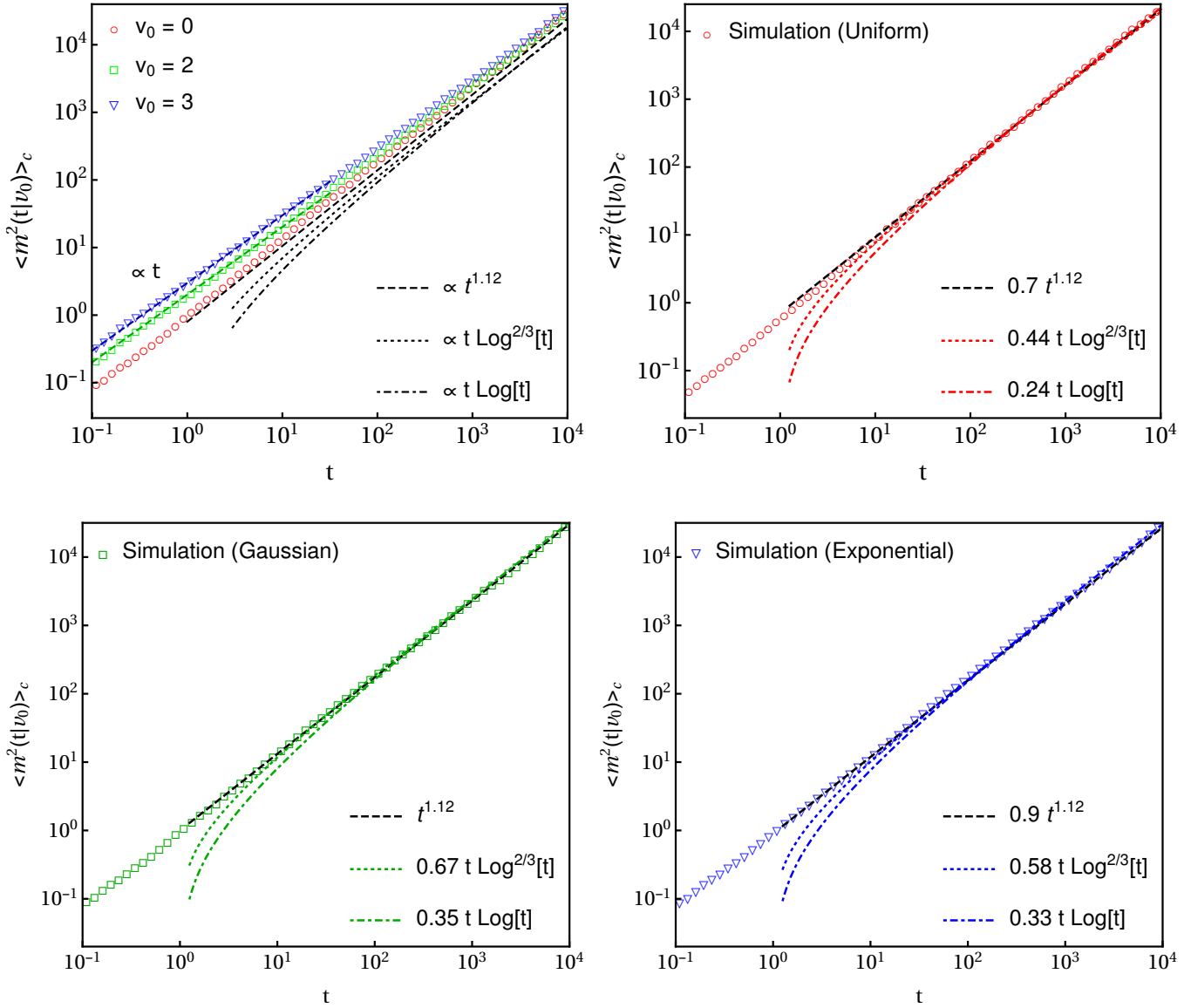


FIG. 4: Simulation results for the variance of the displacement of the tagged particle for the $\alpha = 1$ case discussed in the main text. In the first figure on first row, we plot the variance for three different values of the tagged velocity, while the velocities of the other particles are drawn independently from a symmetric Gaussian distribution. The finite size effects do not show up till the final measurement time considered in the simulations, for a system of size $N = 10^4$ with periodic boundary condition. The data for the largest tagged velocity $v_0 = 3$ shows only a linear growth $\propto t$ in time. The data for the intermediate value $v_0 = 2$ is showing a transition from the initial $\propto t$ behavior to an anomalous long-time behavior. For $v_0 = 0$ an anomalous growth is clearly noticeable. In the second figure on the first row and the first and second figures on the second row, we plot the variance of a tagged particle of velocity $v_0 = \langle v \rangle$ for uniform, Gaussian and exponential distributions respectively, highlighting the anomalous growth. The exact anomalous behavior is not clear as it matches with both $\propto t^{1.12}$ (as shown by bold lines) and $\propto t [\text{Log}(t)]^{2\gamma}$. Our simulation results show good agreement for both $\gamma = 1/3$ (as shown by dotted lines) and $\gamma = 1/2$ (as shown by dot-dashed lines).

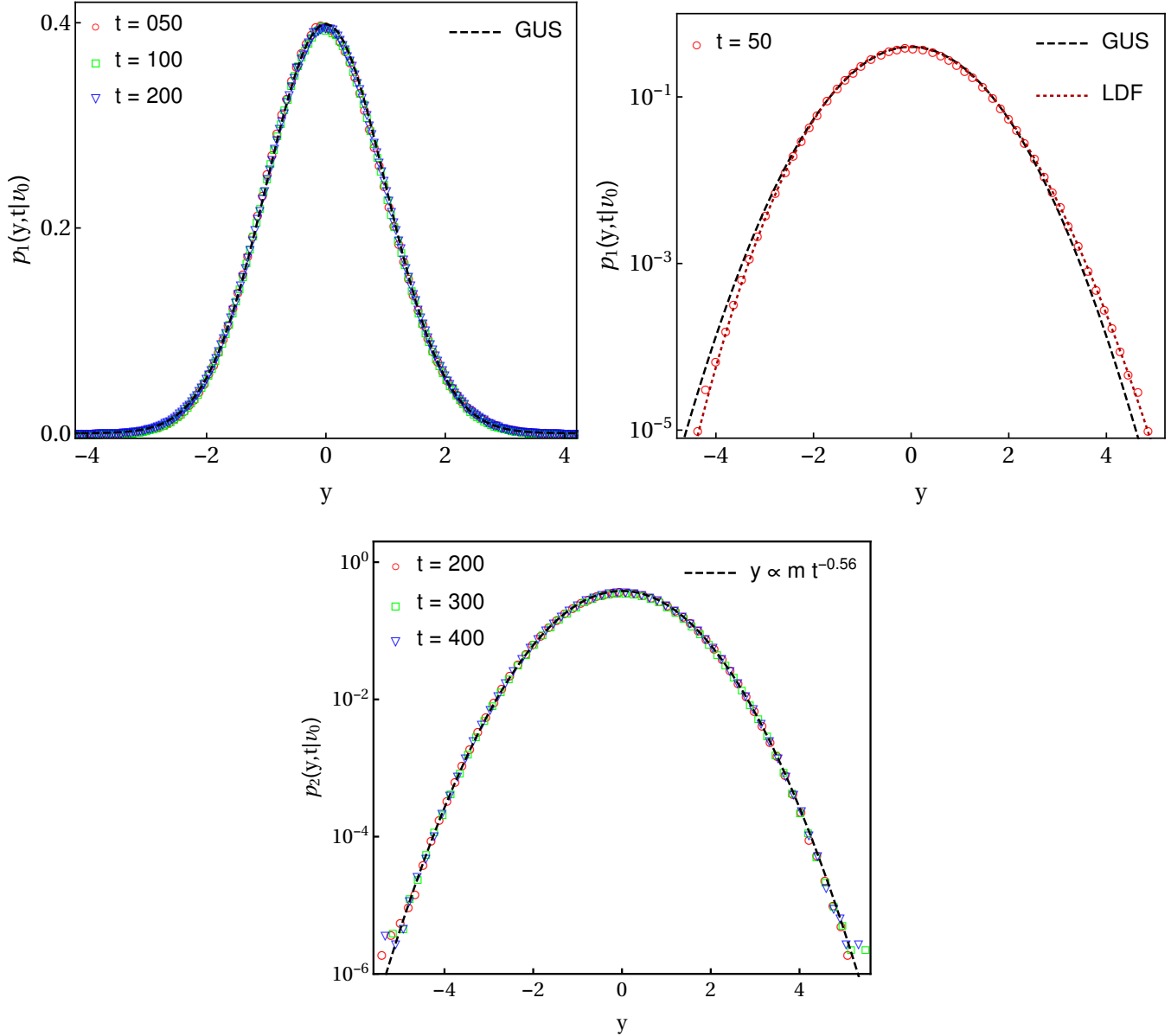


FIG. 5: Conditional PDF of the displacement of a tagged particle with a given velocity in the two different limits (i) $t \ll t_{\#}(v_0)$ (figures on the first row) and (ii) $t \gg t_{\#}(v_0)$ (the figure on the second row), for the $\alpha = 1$ case discussed in the main text. To satisfy these limits we conveniently consider the tagged velocity $v_0 = 3$ and 0 , respectively, while drawing the rest of the velocities independently from a Gaussian distribution. In the first figure on the first row, the typical fluctuations of the scaled displacement $y \propto (m - \bar{c}t)/\sqrt{t}$ are Gaussian (shown by the dashed line) while the second figure on the first row shows that the large fluctuations are better described by a large deviation result (shown by the dotted line, where the dashed line plots the Gaussian distribution). In the figure on the second row, we consider the large time limit $t \gg t_{\#}(v_0)$, where the PDFs of the appropriately scaled displacement $y \propto t^{-0.56}(m - \bar{c}t)$, at three different times collapse onto a Gaussian distribution shown by dashed line. As discussed in Fig. 4 and shown next in Fig. 6, the exact anomalous scaling is not very clear.

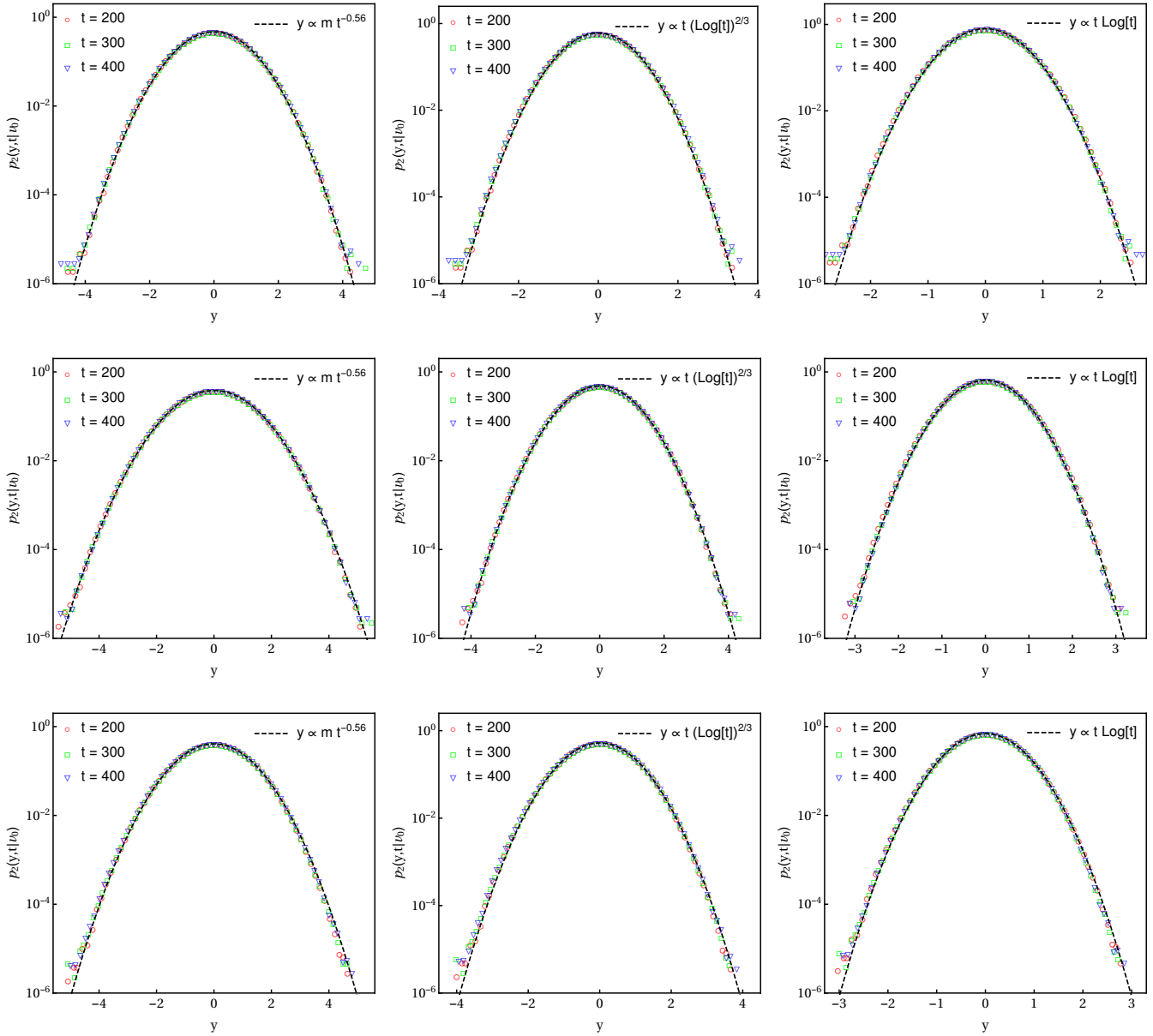


FIG. 6: Conditional PDF of the displacement of a tagged particle with a given velocity $v_0 = \langle v \rangle$, at times $t \gg t_\#$, for the $\alpha = 1$ case discussed in the main text. The velocities of the remaining particles are drawn from three different distributions: uniform (first row), Gaussian (second row) and exponential (third row). While the fluctuations of the scaled displacement $y \propto (m - \bar{c}t)/\sigma_t$ is well described by Gaussian (shown by dashed lines), the exact time dependence of the variance is not clear as it matches equally well with $\sigma_t^2 \propto t^{1.12}$ (figures on the first column) as well as $\sigma_t^2 \propto t [\text{Log}(t)]^{2\gamma}$ for $\gamma = 1/3$ (figures on the second column) and $\gamma = 1/2$ (figures on the third column).

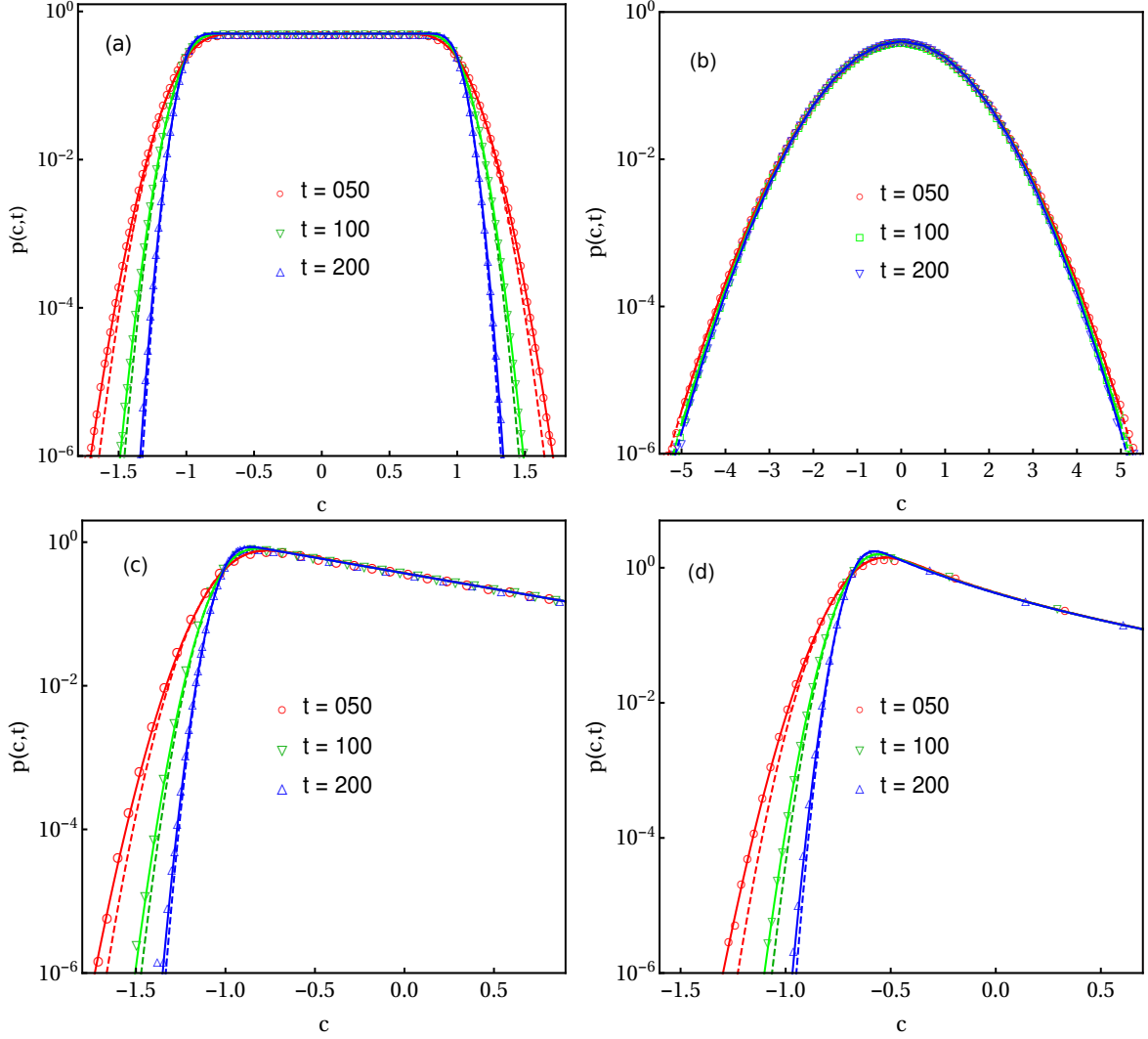


FIG. 7: Probability density function $p(c,t)$ of the scaled net overtakings $c = m(t)/t$ are plotted at three different times, for $\alpha = 1$ case discussed in the main text, with four different choices of the initial velocity distribution, namely, (a) uniform (b) Gaussian (c) exponential and (d) power-law distributions. The discrete points in each plot are the simulation results. They show very good agreement with the results coming from the analysis of the large deviation form of the conditional distribution $p_1(c,t|v_0)$ (as shown by the bold lines). The corresponding results coming from the Gaussian approximation are also plotted (as shown by the dashed lines), for which the agreements at the tails improve as t becomes larger.